



Fractional order dynamics in a GA planner

E.J. Solteiro Pires^{a,*}, J.A. Tenreiro Machado^b, P.B. de Moura Oliveira^a

^aUniv. Trás-os-Montes e Alto Douro, Dep. de Engenharia Electrotécnica Vila Real 5000-911, Portugal

^bInstituto Superior de Engenharia do Porto, Dep. de Engenharia Electrotécnica Rua Dr. António Bernardino de Almeida
Porto 4200-072, Portugal

Received 13 January 2003

Abstract

This work addresses the signal propagation and the fractional-order dynamics during the evolution of a genetic algorithm (GA), for generating a robot manipulator trajectory. The GA objective is to minimize the trajectory space/time ripple without exceeding the torque requirements. In order to investigate the phenomena involved in the GA population evolution, the mutation is exposed to excitation perturbations and the corresponding fitness variations are evaluated. The chaos-like noise and the input/output signals are studied revealing a fractional-order dynamics, characteristic of a long-term system memory. © 2003 Elsevier B.V. All rights reserved.

Keywords: Signal analysis; Fractional calculus; Genetic algorithms; Robotic manipulators; Trajectory planning; Optimization

1. Introduction

This article addresses two apparently distinct areas, namely genetic algorithms (GAs) and fractional calculus (FC). While GAs are a relatively recent, and a well known, field of research, FC is as old as the classical theory of differential calculus, but is still far from being well known in the scientific community.

GAs were developed in the last decade and applied in a large number of fields such as in image processing, pattern recognition, speech recognition, control, system identification, optimization, planning and scheduling [2].

In robotics several GA-schemes for trajectory planning were proposed. A possible approach consists in adopting the differential inverse kinematics for generating the manipulator trajectories [3,6]. However, the algorithm must take into account the problem of kinematic singularities that may be hard to tackle. To avoid this problem, other methods for the trajectory generation are based on the direct kinematics [7,11,23,26,27,32].

In this area of research we can mention also several other studies. Chen and Zalzal [3] proposed an inverse kinematic GA to generate the position and configuration of a mobile robot, optimizing the least torque norm, the manipulability, the torque distribution and the obstacle avoidance.

Davidor [6] also applied GAs to the trajectory generation by searching the inverse kinematics solutions to pre-defined end-effector robot paths.

Rana and Zalzal [23] developed a method to plan a near time-optimal collision-free motion in the case of

* Corresponding author.

E-mail addresses: epires@utad.pt (E.J. Solteiro Pires), jtm@dee.isep.ipp.pt (J.A. Tenreiro Machado), oliveira@utad.pt (P.B. de Moura Oliveira).

¹ Partially supported by the grant Prodep III from FSE.

multi-arm manipulators. The planning is carried out in the joint space and the path is represented as a *string* of via-points connected through cubic splines.

Kubota et al. [11] studied a hierarchical trajectory planning method for a redundant manipulator using a virus-evolutionary GA. This method runs, simultaneously, two processes. One process calculates some manipulator collision-free positions and the other generates a collision-free trajectory by combining these intermediate positions.

On the other hand, the area of fractional calculus (FC) is a natural extension of the classical mathematics and, since the beginning of the theory of differential and integral calculus, many mathematicians investigated the calculation of non-integer order derivatives and integrals. Nevertheless, the application of FC has been scarce until recently, but the advances in the theory of chaos motivated a renewed interest in this field.

The fundamental aspects of the FC theory are addressed in [8,15,16,22,24,25].

In what concerns the FC application we can mention research on viscoelasticity/damping, chaos/fractals, biology, electronics, signal processing, diffusion and wave propagation, percolation, modeling, control and irreversibility [1,4,5,10,12,13,17–21,28,29,31,33].

Bearing these ideas in mind, this paper analyzes the system signal evolution and the fractional-order dynamics in the population of a GA-based trajectory planning scheme for mechanical manipulators. The article is organized as follows. Section 2 introduces the problem, the GA method for its resolution and a run-out experiment, respectively. Based on this formulation, Section 3 presents the results for several simulations involving different excitation conditions and studies the resultant signals and dynamic phenomena. Finally, Section 4 outlines the main conclusions.

2. The GA trajectory planning scheme

This section presents the GA planning scheme to render an optimized trajectory, having a reduced ripple in the space/time evolution, while not exceeding a maximum pre-defined torque. We consider a two-link manipulator, that is required to move between two points in the workspace, and a GA that uses the direct kinematics to avoid singularity problems.

2.1. Trajectory representation

The manipulator can move between two points of the workspace. Therefore, the initial and final configurations are given by the inverse kinematic equations. The path is encoded directly, using real codification, as strings in the joint space to be used by the GA as

$$[\Delta t, (q_{11}, q_{21}), \dots, (q_{1j}, q_{2j}), \dots, (q_{1m}, q_{2m})]. \quad (1)$$

The i th joint variable for a robot intermediate j th position is q_{ij} , the chromosome is constituted by m genes (configurations) and each gene has two values. The joint variables q_{ij} are initialized in the range $]-\pi, +\pi]$. It is important to note that the initial and final configurations have not been encoded into the string because this configuration remains unchanged throughout the trajectory search. Moreover, the additional parameter Δt is introduced in the chromosome to specify the time between two consecutive configurations.

2.2. Operators in genetic algorithm

The initial population of strings is generated at random and the search is then carried out among this population. The evolution of the population elements is non-generational, meaning that the new replace the worst elements. The main different operators adopted in the GA are reproduction, crossover and mutation.

In what concerns the reproduction operator, the successive generations of new strings are generated based on their fitness values. In this case, a 5-tournament [9,14] is used to select the strings for reproduction. Furthermore, another 5-tournament selection is used to choose the strings to be replaced by the children strings.

For the crossover operator it is adopted the single point technique and, therefore, the crossover point is only allowed between genes or, in other words, the crossover operator cannot disrupt genes.

The mutation operator replaces one gene value x_t with a given probability p_m . The new value x_{t+1} is obtained by the equation $x_{t+1} = x_t \pm N[0, (2\pi)^{-1/2}]$, where N represents the Normal probability distribution.

2.3. Evolution criteria

Five indices are used to qualify the evolving trajectory robotic manipulators. All indices are translated

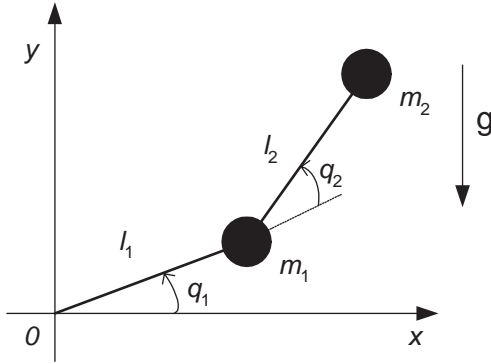


Fig. 1. The two link manipulator.

into penalty functions to be minimized. Each index is computed individually and is integrated in the fitness function evaluation.

The fitness function f adopted for evaluating the candidate trajectories is defined as

$$f = \beta_1 f_{ot} + \beta_2 \dot{q} + \beta_3 \ddot{q} + \beta_4 \dot{p} + \beta_5 \ddot{p}, \quad (2)$$

where the indices f_{ot} , \dot{q} , \ddot{q} , \dot{p} , \ddot{p} are defined in the sequel. The optimization goal consists in finding a set of design parameters that minimize f according to the priorities given by the weighting factors β_i ($i = 1, \dots, 5$).

The f_{ot} index represents the amount of excessive driving, in relation to the maximum torque $\tau_{i \max}$, that is demanded for the i th joint motor for the trajectory under consideration.

$$f_{ot} = \sum_{j=1}^m (f_1^j + f_2^j), \quad (3a)$$

$$f_i^j = \begin{cases} 0, & |\tau_i^j| < \tau_{i \max}, \\ |\tau_i^j| - \tau_{i \max}, & \text{otherwise.} \end{cases} \quad (3b)$$

The dynamic equations of the two link manipulator (Fig. 1) can be easily obtained from the Lagrangian yielding [30]:

$$\tau_1 = d_1 \ddot{q}_1 + d_c \ddot{q}_2 - c \dot{q}_2^2 - 2c \dot{q}_1 \dot{q}_2 + g_1, \quad (4a)$$

$$\tau_2 = d_c \ddot{q}_1 + d_2 \ddot{q}_2 + c \dot{q}_1^2 + g_2, \quad (4b)$$

$$d_1 = m_1 l_1^2 + m_2 [l_1^2 + l_2^2 + 2l_1 l_2 \cos(q_2)], \quad (4c)$$

$$d_2 = m_2 l_2^2, \quad (4d)$$

$$d_c = m_2 [l_2^2 + 2l_1 l_2 \cos(q_2)], \quad (4e)$$

$$c = m_2 l_1 l_2 \sin(q_2), \quad (4f)$$

$$g_1 = g(m_1 + m_2) l_1 \cos(q_1) + g_2, \quad (4g)$$

$$g_2 = g m_2 l_2 \cos(q_1 + q_2). \quad (4h)$$

The joint velocities are used to minimize the manipulator traveling distance yielding the criteria:

$$\dot{q} = \sum_{j=1}^m \sum_{i=1}^2 \dot{q}_{ij}^2. \quad (5)$$

This equation is used to optimize the traveling distance because, if the curve length is minimized, the ripple in the space trajectory is indirectly reduced. For a function $y = g(x)$ the distance curve length is $\int [1 + (dg/dt)^2] dx$ and, in this perspective, to minimize the distance curve length the simplified expression $\int (dg/dt)^2 dx$ is adopted. The fitness function maintains the quadratic terms so that the robot configurations are uniformly distributed between the initial and final configurations.

The joint accelerations are used to minimize the ripple in the time evolution of the robot trajectory through the criteria:

$$\ddot{q} = \sum_{j=1}^m \sum_{i=1}^2 \ddot{q}_{ij}^2. \quad (6)$$

The cartesian velocities are introduced in the fitness function f to minimize the total trajectory length, from the initial point up to the final point. This criterion is defined as

$$\dot{p} = \sum_{j=2}^m d(p_j, p_{j-1})^2, \quad (7)$$

where p_j is the robot j intermediate arm Cartesian position and $d(\cdot, \cdot)$ is a function that gives the distance between the two arguments.

The cartesian acceleration in the fitness functions is responsible for reducing the ripple in time evolution of the arm velocities. This index is formulated as

$$\ddot{p} = \sum_{j=3}^m |d(p_j, p_{j-1}) - d(p_{j-1}, p_{j-2})|^2. \quad (8)$$

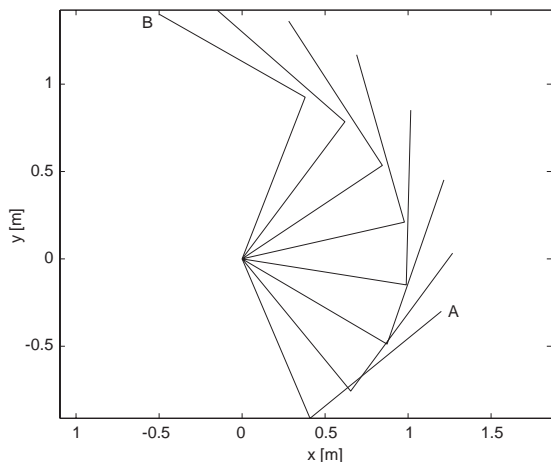


Fig. 2. Robot trajectory in the $\{x, y\}$ plane.

2.4. Simulation results

This simple experiment consists on moving a robotic arm from the starting point $A \equiv \{1.25, -0.30\}$ up to the final point $B \equiv \{-0.50, 1.40\}$. The GA adopts a crossover probability $p_c = 0.8$ per chromosome, a mutation probability $p_m = 0.05$ per locus, a population of 200 elements for the intermediate arm configurations, a string size of $m = 7$ and a 5-tournament selection scheme. The robot links have length and mass of $l_i = 1$ m and $m_i = 1$ kg ($i = 1, 2$), respectively. Moreover, the joints 1 and 2 are free to rotate 2π with maximum allowed torques of $\tau_{1\max} = 16$ Nm and $\tau_{2\max} = 5$ Nm, respectively.

In this study we have two distinct time variables namely, the trajectory time t , during which the arm moves, and the evolution time T , that corresponds to the GA successive generations. In the first case, the time between two consecutive configurations is restricted to the interval $0.05 \leq \Delta t \leq 1.60$ s. In the second case, the normalized time between two consecutive GA generations is considered $T = 1$ s, without losing generality, because it is always possible to perform a time re-scaling.

Figs. 2–5 show the manipulator trajectories in the $\{x, y\}$ plane and the joint positions, velocities and torques, respectively. Fig. 6 depicts the percentiles P_n , $n = \{0, 30, 70, 100\}\%$, of the GA-population fitness throughout the evolution.

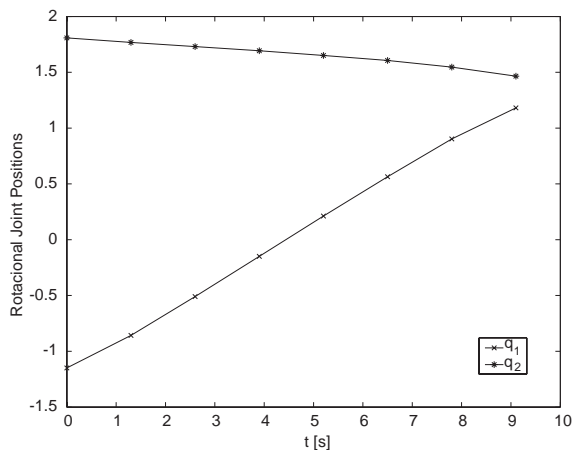


Fig. 3. Robot joint positions vs. time t .

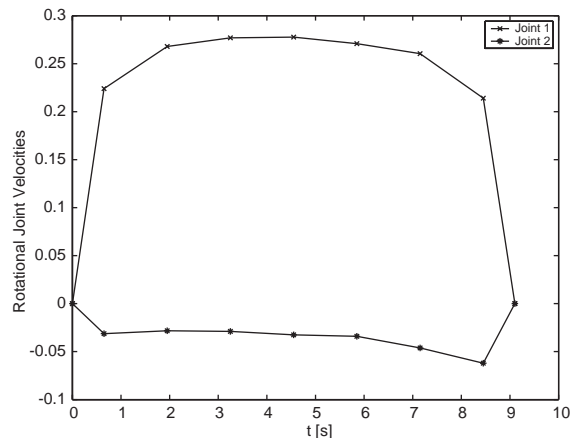


Fig. 4. Robot joint velocities vs. time t .

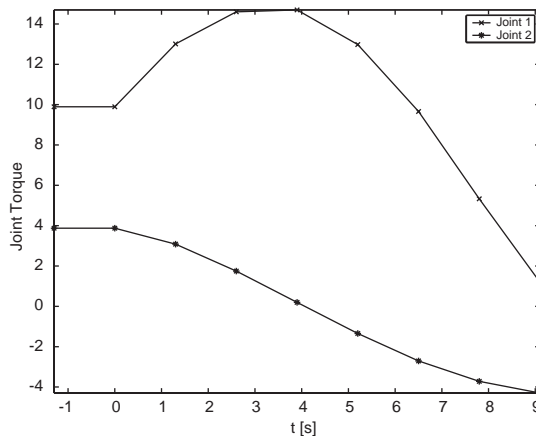


Fig. 5. Robot torque vs. time t .

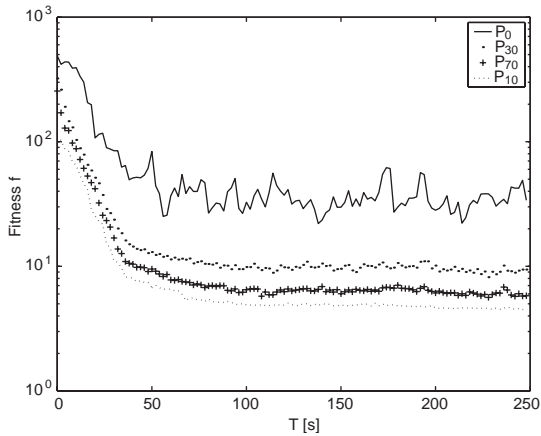


Fig. 6. Percentiles of the population fitness vs. generations T .

The trajectory presents a smooth behavior, both in space and time and the required joint torques do not exceed the imposed limitations.

3. Evolution, signal propagation and fractional-order dynamics

This section studies the dynamical phenomena involved in the signal propagation in the GA population. In this perspective, small amplitude perturbations are superimposed over biasing signals of the GA system and its influence on the population fitness is evaluated. The experiments reveal a fractional-order dynamics and signals behavior with characteristics that resemble those appearing in many chaotic systems.

3.1. Introduction to fractional calculus

Since the foundation of the differential calculus the generalization of the concept of derivative and integral to a non-integer order α has been the subject of distinct approaches. Due to this reason there are several alternative definitions of fractional derivatives. For example, the Laplace definition of a derivative of fractional order $\alpha \in \mathbb{C}$ of the signal $x(t)$, $D^\alpha[x(t)]$, is a ‘direct’ generalization of the classic integer-order scheme yielding:

$$L\{D^\alpha[x(t)]\} = s^\alpha X(s). \tag{9}$$

This means that frequency-based analysis methods have a straightforward adaptation.

An alternative approach, based on the concept of fractional differential, is the Grünwald–Letnikov definition given by

$$D^\alpha[x(t)] = \lim_{h \rightarrow 0} \frac{1}{\Gamma(\alpha)h^\alpha} \sum_{k=0}^{\lfloor \frac{x-a}{h} \rfloor} \frac{\Gamma(\alpha+k)}{\Gamma(k+1)} x(t-kh). \tag{10}$$

An important property revealed by this equation is that while an integer-order derivative implies just a finite series, the fractional-order derivative requires an infinite number of terms. This means that integer derivatives are ‘local’ operators in opposition with fractional derivatives that have, implicitly, a ‘memory’ of all past events.

The characteristics revealed by fractional-order models make this mathematical tool well suited to describe phenomena such as irreversibility and chaos due to its inherent memory property. In this line of thought, the propagation of perturbations and the appearance of long-term dynamic phenomena in a population of individuals subjected to an evolutionary process seem to be a case where FC tools fit adequately.

3.2. Simulations

In this section the GA system is stimulated by perturbing the mutation probability through a white noise signal and the corresponding population fitness modification is evaluated. Therefore, the variation of the mutation probability and the resulting fitness modification on the GA population, during the evolution, can be viewed as the system inputs and output signals versus time, respectively.

The excitation signal has small amplitude and ‘acts’ upon the GA-system during a time period T_{exc} . In this perspective, a white noise signal Δp is added to the mutation probability p_m of the joint variables genes and the new mutation probability p_{m_noise} is calculated by the following formula:

$$p_{m_noise} = \begin{cases} 0, & p_m + \Delta p < 0, \\ 1, & p_m + \Delta p > 1, \\ p_m + \Delta p, & \text{otherwise.} \end{cases} \tag{11}$$

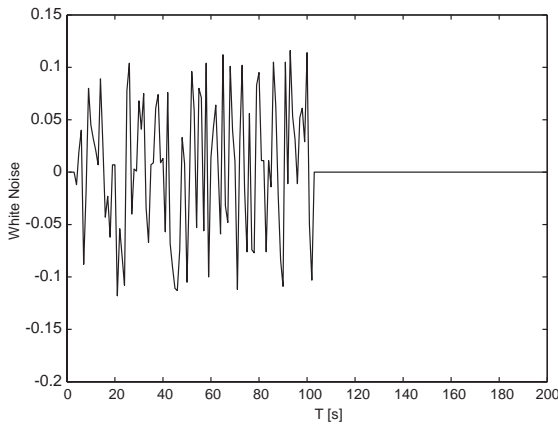


Fig. 7. Input perturbation $\delta p_m(T)$ injected in the mutation probability during $T_{exc} = 100$ generations.

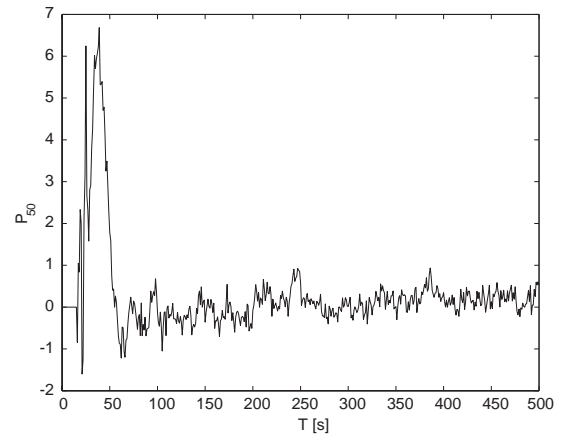


Fig. 9. Output percentile variation $\delta P_{50}(T)$ for an input excitation over $T_{exc} = 100$ generations.

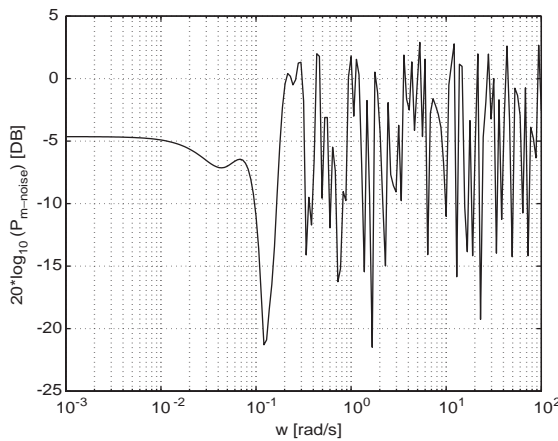


Fig. 8. Fourier spectrum $F\{\delta p_m(T)\}$ of the mutation probability variation.

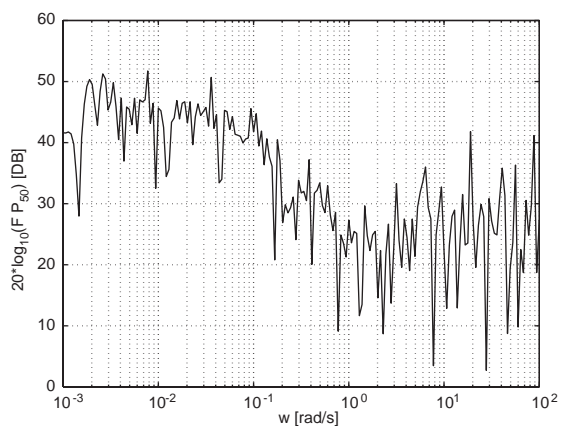


Fig. 10. Fourier spectrum $F\{\delta P_{50}(T)\}$ of the fitness function $n = 50\%$ percentile variation.

Consequently, the input signal is the difference between the two cases, that is $\delta p_m(T) = p_{m_noise}(T) - p_m(T)$. On the other hand, the output signals are the difference in the population fitness n -percentiles with and without noise, that is $\delta P_n(T) = P_{n_noise}(T) - P_n(T)$.

Figs. 7 and 8 show the input signal δp_m , in the time and frequency domains, for a $\Delta p = 0.12 p_m$ perturbation in the mutation probability and an excitation period of $T_{exc} = 100$ generations. Figs. 9 and 10 show the corresponding output signal variation δP_{50} , for the percentile $n = 50\%$ of the fitness function. The transfer function $H_n(j\omega)$, between the input and output

signals, and the fractional order analytical approximation $G_n(j\omega)$ are depicted in Fig. 11.

3.3. Identification

In this section, the numerical data of the system transfer functions are approximated by analytical expressions with gain $k \in \mathfrak{R}$, one zero and one pole $(a, b) \in \mathfrak{R}$ of fractional orders $(\alpha, \beta) \in \mathfrak{R}$, respectively, given by

$$G_n(s) = k \frac{(s/a)^\alpha + 1}{(s/b)^\beta + 1}. \tag{12}$$

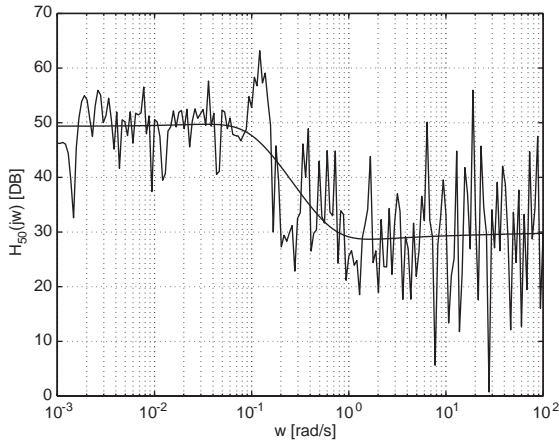


Fig. 11. Transfer function $H_{50}(j\omega)=F\{\delta P_{50}(T)\}/F\{\delta p_m(T)\}$ and the analytical approximation $G_{50}(j\omega)$ for the percentile $n = 50\%$.

A GA adopting a real string identifies the $G_n(s)$ parameters using the representation $[k, a, b, \alpha, \beta]$.

The main operators are identical to those deployed in Section 2.2 but, when one mutation occurs the corresponding value $\{x_1, \dots, x_5\} \equiv \{k, a, b, \alpha, \beta\}$ is changed according with the equations:

$$x_{i+1} = 10^{u_i} x_i \tag{13a}$$

$$u_i \sim U[-\varepsilon_i, +\varepsilon_i] \tag{13b}$$

where u_i is a random number generated through the uniform probability distribution U and ε_i is fixed according to the range of estimation. In Eq. (13a) it is adopted an exponential adjusting procedure because the estimation is carried out in a logarithm scale.

The fitness function $f_{n,ide}$ measures, logarithmically, the distance between the numerical H_n and the analytical G_n transfer functions:

$$f_{n,ide} = \sum_{i=1}^{nf} \left[\log_{10} \frac{H_n(\omega_i)}{G_n(\omega_i)} \right]^2 \tag{14}$$

$$G_n(\omega_i)$$

$$= k \left\{ \frac{\left[\left(\frac{\omega_i}{a} \right)^\alpha \cos\left(\frac{\pi}{2} \alpha\right) + 1 \right]^2 + \left[\left(\frac{\omega_i}{a} \right)^\alpha \sin\left(\frac{\pi}{2} \alpha\right) \right]^2}{\left[\left(\frac{\omega_i}{b} \right)^\beta \cos\left(\frac{\pi}{2} \beta\right) + 1 \right]^2 + \left[\left(\frac{\omega_i}{b} \right)^\beta \sin\left(\frac{\pi}{2} \beta\right) \right]^2} \right\}^{1/2} \tag{15}$$

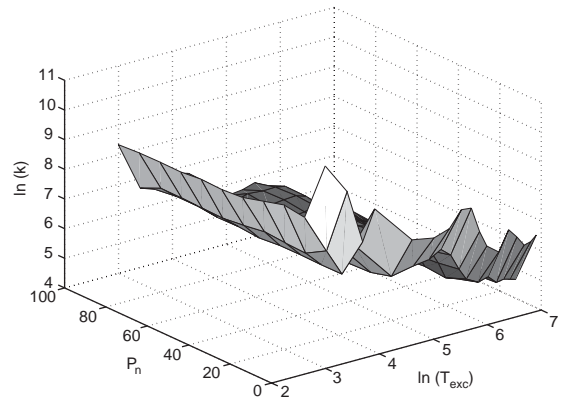


Fig. 12. Estimated gain $\ln(k)$ vs. (T_{exc}, P_n) .

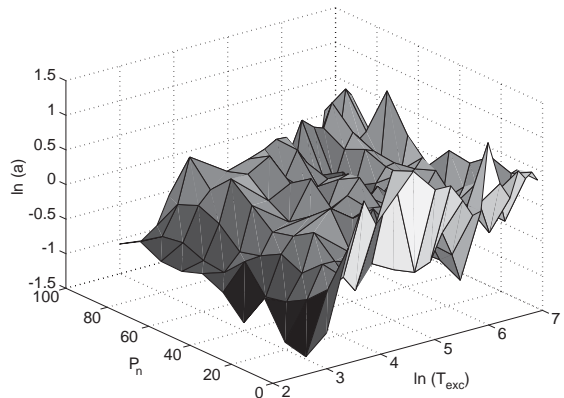


Fig. 13. Estimated zero $\ln(a)$ vs. (T_{exc}, P_n) .

where nf is the total number of sampling points in the frequency domain and $\omega_i, i = 1, \dots, nf$, is the corresponding vector of frequencies.

In order to obtain the parameters of expression (12) twenty one GA identification tests are performed and the medians of the results are adopted as the final estimated parameters. Moreover, for evaluating the influence of the excitation period T_{exc} several simulations are performed ranging from $T_{exc} = 20$ to 1000 generations. The relation between the transfer function parameters and (T_{exc}, P_n) are shown in Figs. 12–16.

The charts of $\{k, a, b, \alpha, \beta\}$ can be approximated through a least squares technique leading to

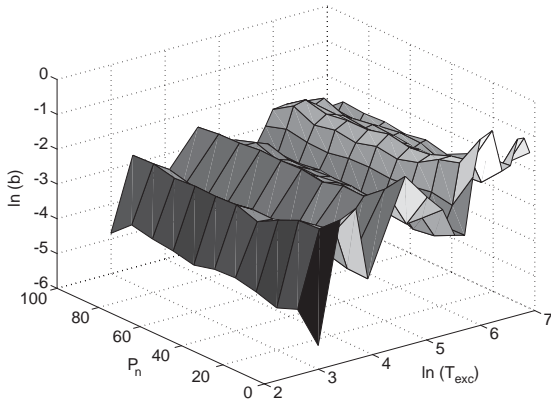


Fig. 14. Estimated pole $\ln(b)$ vs. (T_{exc}, P_n) .

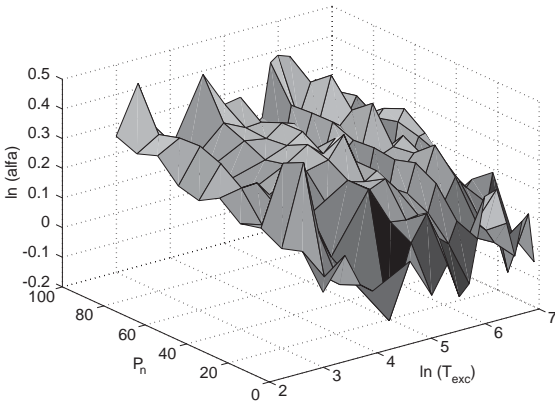


Fig. 15. Estimated zero fractional-order $\ln(\alpha)$ vs. (T_{exc}, P_n) .

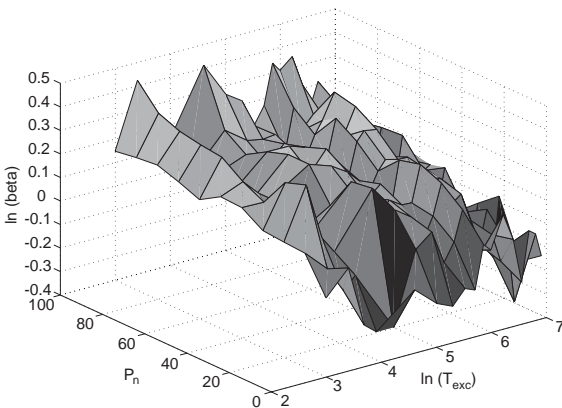


Fig. 16. Estimated pole fractional-order $\ln(\beta)$ vs. (T_{exc}, P_n) .

the equations:

$$k = 62069 T_{exc}^{0.852} e^{-0.011P_n}, \tag{16a}$$

$$a = 0.317 T_{exc}^{0.204} e^{-0.0044P_n}, \tag{16b}$$

$$b = 0.012 T_{exc}^{0.362} e^{-0.0060P_n}, \tag{16c}$$

$$\alpha = 1.121 T_{exc}^{-0.005} e^{0.0019P_n}, \tag{16d}$$

$$\beta = 1.093 T_{exc}^{-0.028} e^{0.0025P_n}. \tag{16e}$$

These results reveal that the transfer function parameters have a low dependence on the percentile P_n of the fitness function and, consequently, that the adoption of a particular value for n is of no importance for the study under effect. On the other hand, the period of excitation T_{exc} has a much stronger influence on the parameter variation.

By enabling the zero/pole order to vary freely, we get non-integer values for α and β , while the adoption of an integer-order transfer function would lead to a larger number of zero/poles to get the same quality in the analytical fitting to the numerical values. The ‘requirement’ of fractional-order models in opposition with the classical case of integer models is a well-known discussion and even nowadays final conclusions are not clear, since it is always possible to approximate a fractional frequency response through an integer one as long as we make use of a larger number of zeros and poles. Nevertheless, in the present experiments there is a complementary point of view in the direction of FC. In fact, analyzing the output signal, we observe that we have a kind of white noise behavior with similarities to signals appearing in natural systems, that is auto-sustained, even for time periods very far away from the excitation perturbation period. This characteristic is typical of chaotic systems and suggests further research on the signal dynamics that would occur for other input perturbations, that is, for other GA variables and distinct perturbing signal spectra.

4. Conclusions

This paper analyzed the signal propagation and the dynamic phenomena involved in the time evolution of a population of individuals. The study was established

on the basis of a GA for the trajectory planning of robot manipulators. While GA schemes has been extensively studied, the influence of perturbation signals over the operating conditions is not well known.

Bearing these ideas in mind, the fundamental aspects of the FC calculus were introduced in order to develop approximating transfer functions of variable order, either integer or non-integer. It was shown that fractional-order models capture phenomena and properties that classical integer-order simply neglect. Moreover, for the case under study the signal evolution have similarities to those revealed by chaotic systems which confirms the requirement for mathematical tools well adapted to the phenomena under investigation. In this line of thought, this article is a step towards the signal and system analysis based on the theory of FC.

References

- [1] T.J. Anastasio, The fractional-order dynamics of brainstem vestibulo-oculomotor neurons, *Biol. Cybernetics* 72 (1994) 69–79.
- [2] T. Bäck, U. Hammel, Hans-Paul, Schwefel, Evolutionary computation: comments on the history and current state, *IEEE Trans. Evolutionary Comput.* 1 (1) (April 1997) 3–17.
- [3] M. Chen, A.M.S. Zalzalá, A genetic approach to motion planning of redundant mobile manipulator systems considering safety and configuration, *J. Robot. Systems* 14 (7) (1997) 529–544.
- [4] Y.Q. Chen, K.L. Moore, Discretization schemes for fractional-order differentiators and integrators, *IEEE Trans. Circuits and Systems—I: Fundamental Theory Appl.* 49 (3) (March 2002) 363–367.
- [5] J.P. Clerc, A.-M.S. Tremblay, G. Albinet, C.D. Mitescu, A. C. Response of Fractal Networks, *Le J. Phys.-Lett.* 45 (19) (October 1984) L.913–L.924.
- [6] Y. Davidor, *Genetic Algorithms and Robotics, a Heuristic Strategy for Optimization*, World Scientific, Singapore, 1991.
- [7] A.B. Doyle, D.I. Jones, Robot path planning with genetic algorithms, *Proceedings of the 2nd Portuguese Conference on Automatic Control*, Porto, Portugal, September 11–13, 1996, pp. 312–218.
- [8] A. Gement, On fractional differentials, *Philos. Mag.* 25 (1938) 540–549.
- [9] D.E. Goldberg, *Genetic Algorithms in Search, Optimization, and Machine Learning*, Addison-Wesley, Reading, MA, 1989.
- [10] C.G. Koh, J.M. Kelly, Application of fractional derivatives to seismic analysis of base-isolated models, *Earthquake Eng. Struct. Dyn.* 19 (1990) 229–241.
- [11] N. Kubota, T. Arakawa, T. Fukuda, Trajectory generation for redundant manipulator using virus evolutionary genetic algorithm, *Proceedings of the IEEE International Conference on Robotics and Automation*, Albuquerque, New Mexico, April 20–25, 1997, pp. 205–210.
- [12] A. Le Méhauté, *Fractal Geometries: Theory and Applications*, Penton Press, London, 1991.
- [13] S.H. Liu, Fractal model for the ac response of a rough interface, *Phys. Rev. Lett.* 55 (5) (July 1985) 529–532.
- [14] Z. Michalewicz, *Genetic Algorithms + Data Structures = Evolution Programs*, Springer, Berlin, 1996.
- [15] K.S. Miller, B. Ross, *An Introduction to the Fractional Calculus and Fractional Differential Equations*, Wiley, New York, 1993.
- [16] K.B. Oldham, J. Spanier, *The Fractional Calculus: Theory and Application of Differentiation and Integration to Arbitrary Order*, Academic Press, New York, 1974.
- [17] M.D. Ortigueira, Fractional discrete-time linear systems, *Proceedings of the ICASSP'97—IEEE International Conference on Acoustics, Speech and Signal Processing*, Munich, Germany, April 20–24, 1997.
- [18] A. Oustaloup, Fractional order sinusoidal oscillators: optimization and their use in highly linear FM modulation, *IEEE Trans. Circuits Systems* 28 (10) (October 1981) 1007–1009.
- [19] A. Oustaloup, *La commande CRONE: commande Robuste d'Ordre Non Entier*, Hermes, 1991.
- [20] A. Oustaloup, *La Dérivation Non Entier: Théorie, Synthèse et Applications*, Editions Hermes, Paris, 1995.
- [21] H.M. Ozaktas, O. Arikan, M.A. Kutay, G. Bozdagi, Digital computation of the fractional fourier transform, *IEEE Trans. Signal Process.* 44 (9) (September 1996) 2141–2150.
- [22] I. Podlubny, *Fractional Differential Equations*, Academic Press, San Diego, 1999.
- [23] A. Rana, A. Zalzalá, An evolutionary planner for near time-optimal collision-free motion of multi-arm robotic manipulators, *Proceedings of the UKACC International Conference on Control*, Vol. 1, 1996, pp. 29–35.
- [24] B. Ross (Ed.), *Fractional Calculus and its Applications*, *Lecture Notes in Mathematics*, Vol. 457, Springer, Berlin, 1974.
- [25] S.G. Samko, B. Ross, Integration and differentiation to a variable fractional order, *Integral Transform. Special Functions* 1 (4) (1993) 227–300.
- [26] E.J. Solteiro Pires, J.A. Tenreiro Machado, Trajectory optimization for redundant robots using genetic algorithms, *Proceedings of the GECCO 2000—Proceedings of the Genetic and Evolutionary Computation Conference*, Las Vegas, Nevada, USA, July 10–12, 2000, p. 967.
- [27] E.J. Solteiro Pires, J.A. Tenreiro Machado, A GA perspective of the energy requirements for manipulators maneuvering in a workspace with obstacles, *Proceedings of the CEC 2000—Congress on Evolutionary Computation*, San Diego, California, USA, July 16–19, 2000, pp. 1110–1116.

- [28] J.A. Tenreiro Machado, Analysis and design of fractional-order digital control systems, *J. System Anal.-Modell.-Simul.* 27 (1997) 107–122.
- [29] J.A. Tenreiro Machado, System modeling and control through fractional-order algorithms, *J. Fraction. Calculus Appl. Anal.* 4 (2001) 47–66.
- [30] J.A. Tenreiro Machado, J.L. Martins de Carvalho, A.M.S. Galhano, Analysis of robot dynamics and compensation using classical and computed torque techniques, *IEEE Trans. Education.* 36 (4) (November 1993) 372–379.
- [31] P.J. Torvik, R.L. Bagley, On the appearance of the fractional derivative in the behaviour of real materials, *ASME J. Appl. Mech.* 51 (June 1984) 294–298.
- [32] Q. Wang, A.M.S. Zalzal, Genetic control of near time-optimal motion for an industrial robot arm, *Proceedings of the IEEE International Conference on Robotics and Automation*, Minneapolis, Minnesota, April 22–28, 1996, pp. 2592–2597.
- [33] S. Westerlund, *Dead Matter has Memory!* Causal Consulting, Kalmar, Sweden, 2002.